Journal of Imaging Science and Technology® 56(3): 030501-1–030501-17, 2012.

A Novel Confusion-Line Separation Algorithm Based on Color Segmentation for Color Vision Deficiency

Dongil Han and Seong Joon Yoo
Department of Computer Engineering, Sejong University, 98 Gunja-dong, Gwangjin-gu, Seoul, Republic of Korea
E-mail: dihan@sejong.ac.kr

Byungwhan Kim
Department of Electronic Engineering, Sejong University, 98 Gunja-dong, Gwangjin-gu, Seoul, Republic of Korea

Abstract. *This article proposes a confusion-line separation algorithm in a CIELAB color space using color segmentation for protanopia and deuteranopia. Images are segmented into regions by grouping adjacent pixels with similar color information using the hue components of the images. To this end, the region-growing method and the seed points used in this method are the pixels that correspond to peak points in hue histograms. In order to establish a color vision deficiency (CVD) confusion-line map, the authors establish 512 virtual boxes in an RGB 3-D space so that boxes existing on the same confusion line can be easily identified. The authors then check whether segmented regions exist on the same confusion line and perform a color adjustment in a CIELAB color space so that all adjacent regions exist on different confusion lines in order to provide the best color-identification effect for those with CVDs.* © *2012 Society for Imaging Science and Technology.*
[DOI: 10.2352/J.ImagingSci.Technol.2012.56.3.030501]

INTRODUCTION

Thanks to the rapid development of color publishing and color information-display technologies, numerous color-expression methods have recently been developed, ranging from smartphones to ultra-large display devices, enabling people to enjoy more vivid and splendid color information. Unfortunately, those with color vision deficiencies (CVDs) have been alienated, as they are unable to share these pieces of color information. Congenital CVD is one of the most common inherited disorders of vision: its prevalence may be as high as 8% in males and 0.5% in females.[1] Thus, the development of color-correction technology for CVDs is urgently needed. Congenital CVDs are generally classified by severity (anomalous trichromacy, dichromacy, and monochromacy) and may be further classified by the type(s) of cone affected.[1] In this article, we intend to present a color-correction solution for red–green CVD. This term is used to encompass protanomaly, deuteranomaly, protanopia, and deuteranopia, accounting for most of the CVD population.

Color-correction technologies for people with CVDs that have been developed thus far are for color conversion in diverse color spaces, including RGB and CIE Lab, through various methods. The Daltonization method[2] expresses the values of LMSs and globally transfers them using color-conversion matrices. A method proposed by Huang[3] is intended to correct colors naturally in CIE Lab color spaces. Bo Liu et al.[4] once presented recoloring on video frames. In addition, in a recent study by Yu-Chieh Chen, color-correction technology was implemented in real time by hardware.[5]

All of these methods may generate images that are more comprehensible to individuals with CVDs. However, transformed images may look very unnatural to viewers with normal vision. From an application viewpoint, webpage images may be simultaneously observed by individuals with and without color deficiencies.

To solve these problems, in this study, we used a more fundamental approach to developing a color-correction method for people with CVDs while minimizing the region of color correction. First, using the process for simulating color recognition in protanopia and deuteranopia presented in a study by Viénot et al.,[6] we obtained simulation data on color recognition by those with CVDs. Furthermore, we investigated confusion-line maps of color regions through the process of simulating and correcting color recognition by people with CVDs.

Then, in order to increase the legibility of the color information in the images, we segmented the images by hue into several regions and transformed the colors so that all regions of the image were located on different confusion lines. Based on these results, we verified that optimum color-identification effects could be provided to people with CVDs.

CONFUSION-LINE SEPARATION ALGORITHM

Figure 1 presents a block diagram of the entire structure of the color conversion for protanopia and deuteranopia using the color-region segmentation proposed in this article. The proposed algorithm consists of a CIE $L^*c^*_{ab}h_{ab}$ color-space conversion block for extracting h^*_{ab} values in an image, a seed-point creation block for extracting seed points, a color-segmentation block for segmenting regions, a confusion-line judgment block for judging whether the

Received Apr. 21, 2011; accepted for publication Aug. 8, 2012; published online Oct. 22, 2012.
1062-3701/2012/56(3)/030501/17/$20.00

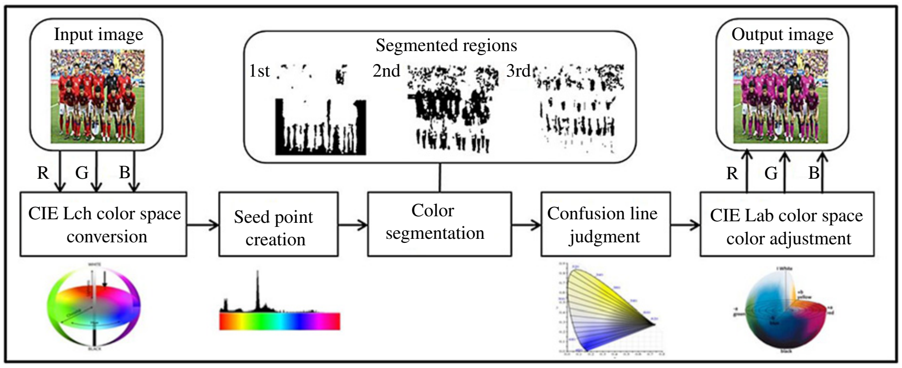

Figure 1. Block diagram of the proposed algorithm.

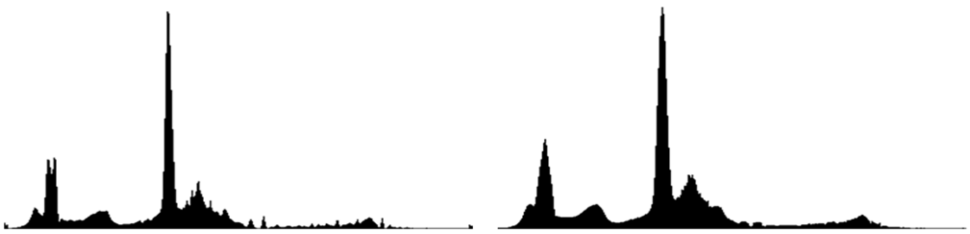

(a) histogram before low-pass filter processing (b) histogram after low-pass filter processing

Figure 2. Hue histogram.

segmented regions are on the same confusion lines, and a CIE L*a*b* color-space color-adjustment block for the color conversion of confusing regions.

CIE Lch color-space conversion block

This is a block for converting R, G, and B image signals in input images into L, C, and H image signals. In order to find the hue values necessary in the color-segmentation block, this block uses CIE L*$c^*_{ab}$$h_{ab}$ color spaces.[7,8] CIE L*$c^*_{ab}$$h_{ab}$ is a polar-coordinate version of CIE L*a*b* as follows:

$$L^* = 116f\left(\frac{Y}{Y_n}\right) - 16 \tag{1}$$

$$a^* = 500\left[f\left(\frac{X}{X_n}\right) - f\left(\frac{Y}{Y_n}\right)\right] \tag{2}$$

$$b^* = 200\left[f\left(\frac{Y}{Y_n}\right) - f\left(\frac{Z}{Z_n}\right)\right] \tag{3}$$

$$\text{where}, f(q) = q^{1/3} \quad for \quad q > 0.008856 \tag{4}$$

$$f(q) = 7.787q + \frac{16}{116} \quad for \quad q \le 0.008856 \tag{5}$$

and Xn, Yn, and Zn are the CIE 1931 tristimulus values of the reference white under the reference illumination. These values are typically the white of a perfectly reflecting diffuser under CIE standard D65 illumination defined by $x = 0.3127$ and $y = 0.3290$ in the CIE chromaticity diagram.[12]

The [a*, b*] pair can be used to express chroma and hue as follows:

$$c^*_{ab} = \sqrt{a^{*2} + b^{*2}} \tag{6}$$

$$h_{ab} = \tan^{-1}\frac{b^*}{a^*}. \tag{7}$$

Seed-point creation block

The seed-point creation block serves the role of extracting the hue that occupies the largest area of each image in order to implement color segmentation. To this end, this block uses the hue information converted in the CIE Lch color-space conversion block to create hue histograms. Then, for accurate hue extraction, this block applies a low-pass filter to the histograms. Figure 2(a) and (b) are the hue histogram results from the Figure 7(a) image. Image 2(a) shows the raw histogram, while image 2(b) shows the hue histogram after the low-pass filter processing. If irregularities are removed through the low-pass filter processing of the hue histogram, smooth histogram results as seen in image 2(b) can be obtained. Through the low-pass filter processing of the hue histogram, a small number of seed points can be created.

Color segmentation

After hue histograms pass through the low-pass filter, they are arranged in descending order of hue values beginning from the hue value having the highest peak. Then, the peak point with the largest value is selected, and an image position that has that hue value is designated as a seed point. Then, the region centering on this point is expanded.[9] Figure 3 shows a flowchart of the color-segmentation algorithm.

First, a point among those points is selected that corresponds to the hue values selected as peak values. Then, similar hue regions in eight directions from the point are searched for. Eqs. (8) and (9) are numerical formulas to

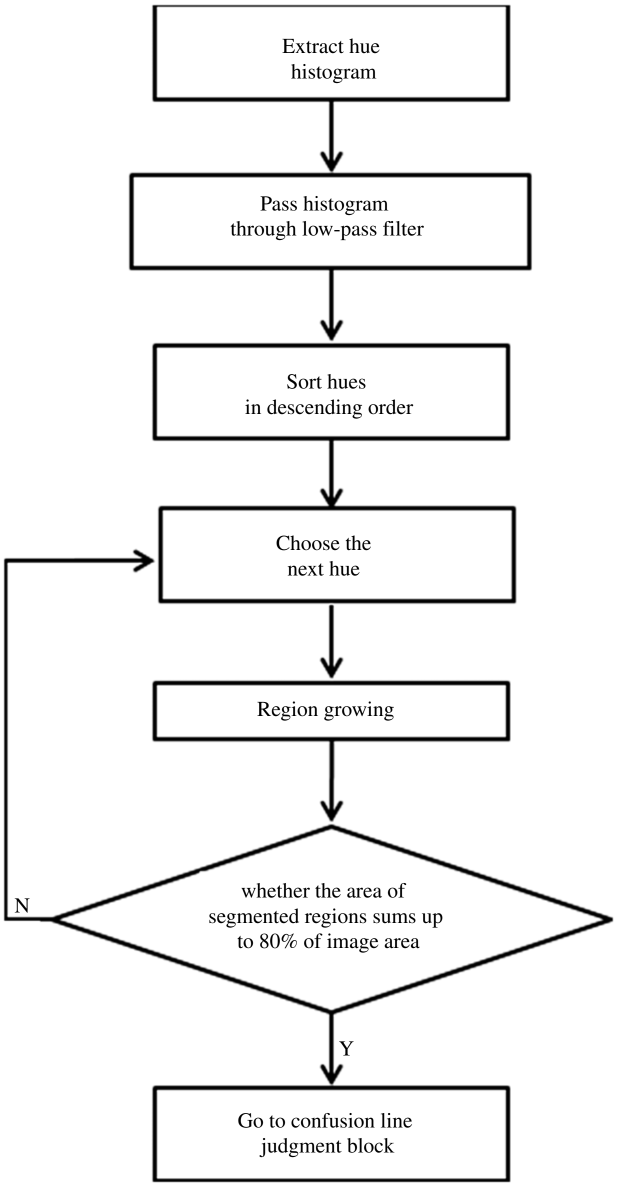

Figure 3. Color-segmentation flowchart.

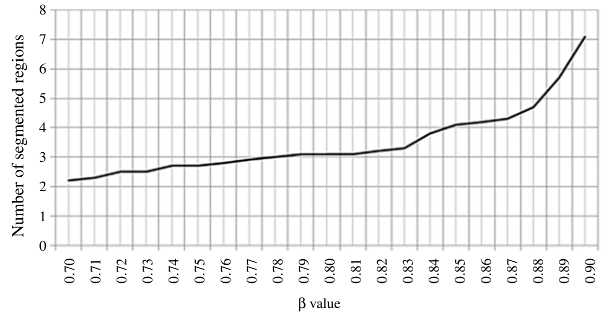

Figure 5. Number of segmented regions with different β values ($\alpha = 0.1$).

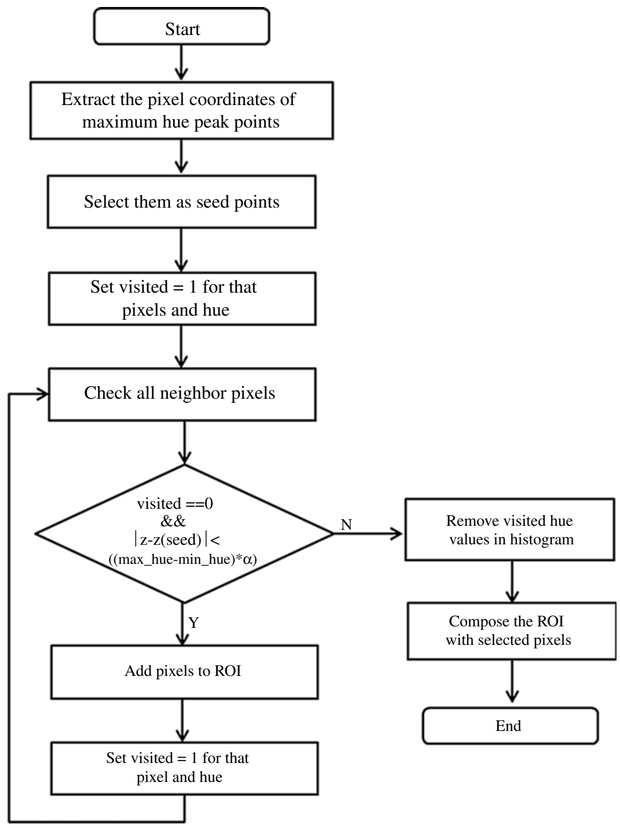

Figure 6. Region-growing flowchart.

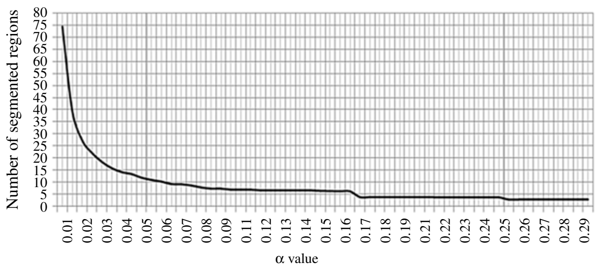

Figure 4. Number of segmented regions with different α values.

search for similar hue regions. If the difference of hue values between the current pixel and reference pixel is less than the threshold value, this pixel can be defined as the same hue region.

In this manner, one keeps searching for the same hue regions using recursive functions and grouping them into the same region. A visit check memory is made and set pixels are visited once to 1 in order to prevent repetition. The peak value is then designated as another seed point, and to perform color segmentation, region growing is performed at those points for pixels recorded as 0 in the visit check memory using the same method.

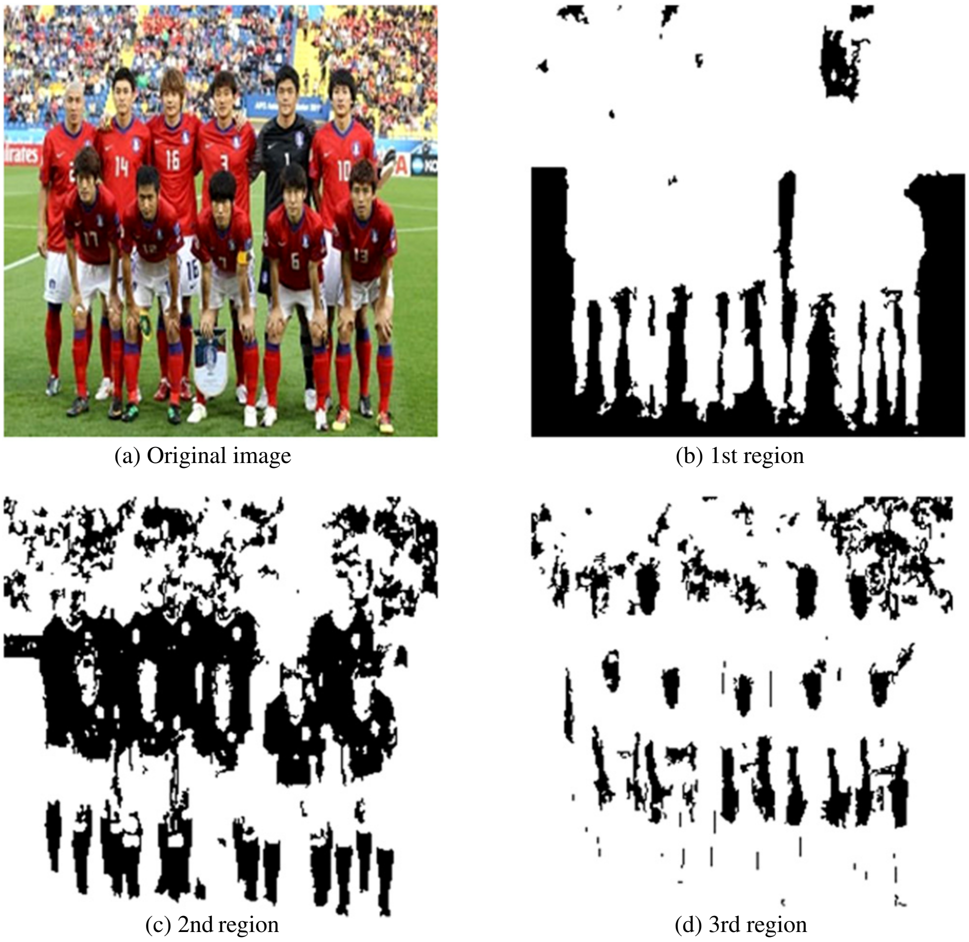

Figure 7. Experimental results of color segmentation.

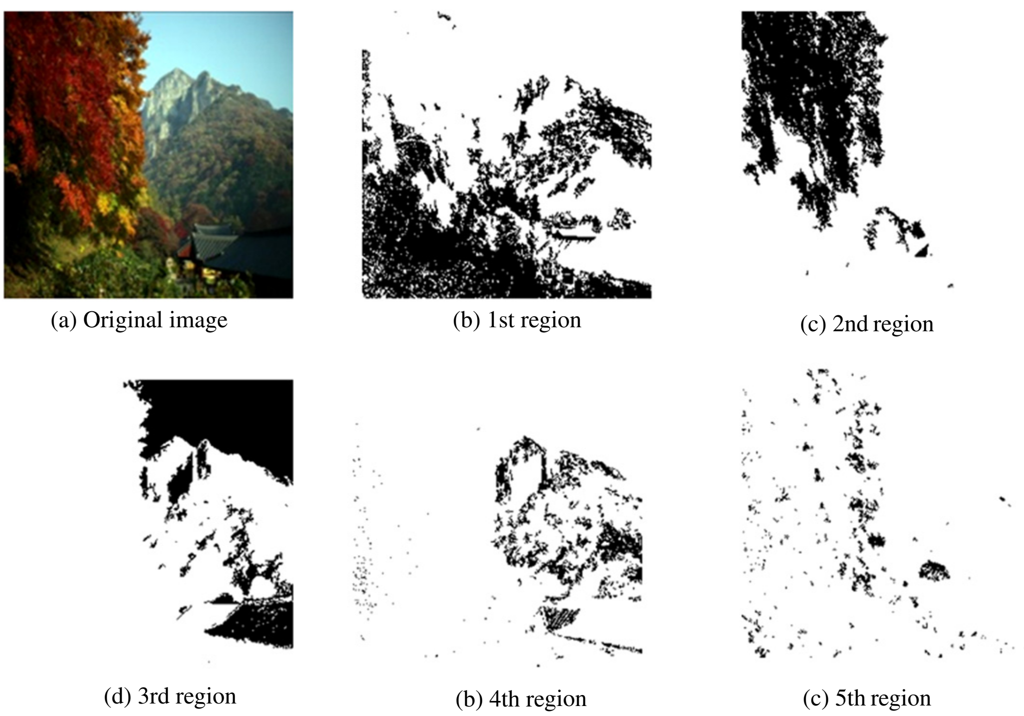

Figure 8. Experimental results of color segmentation.

Table I. Confusion-line map.

Type of CVD	Type of confusion line	Representative box position (R G B)	Box positions in same confusion line (R G B)		
Protanopia	P1	0 0 0	0 0 0	1 0 0	2 0 0
	P2	0 0 1	0 0 1	1 0 1	2 0 1
		≈			
	P52	7 7 7	0 7 7	≈	7 7 7
Deuteranopia	D1	1 1 1	0 0 0	≈	2 1 1
	D2	1 1 2	0 0 2	≈	2 1 2
		≈			
	D41	4 7 7	2 7 7	3 7 7	4 7 7

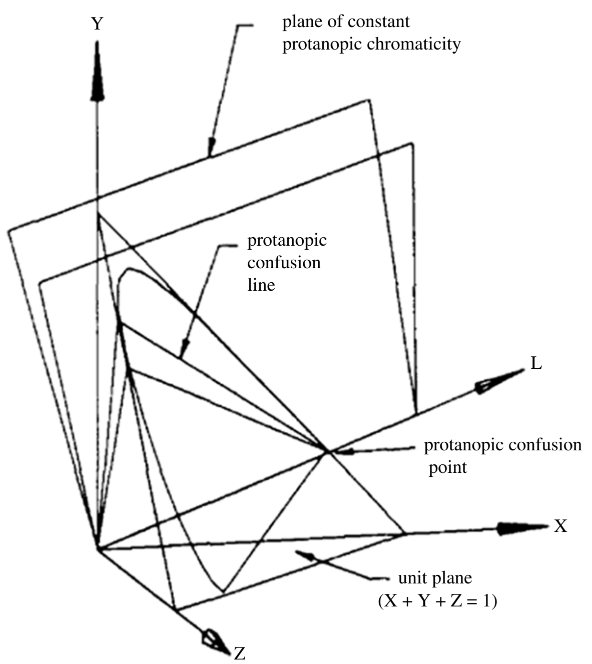

Figure 9. Confusion lines in the CIE XYZ space.

Finally, if the sum of segmented regions R1, R2, R3, …, Rn is 80% or more of the entire input image, as shown in numerical equation (10), the region segmentation is finished.

$$|\, z - z\_seed \,| < hue\_threshold \quad (8)$$

$$hue\_threshold = |\max\_hue - \min\_hue| * \alpha \quad (9)$$

$$\sum_{i=0}^{n} Ri > R * \beta. \quad (10)$$

Figure 4 shows the number of segmented regions based on the choice of α value in Eq. (9). As α approaches 0, the number of segmented regions increases unnecessarily. When α is near 0.1, the number of generated regions remains constant and coincides with human decision-making. Figure 5 shows the number of segmented regions based on the choice of β value in Eq. (10). Here, the α value is set to 0.1. As β approaches 1, the number of segmented regions also increases unnecessarily. In this article, α as defined as 0.1 and β as 0.8.

Figure 6 shows a flowchart of the region-growing algorithm used in this study. Through a series of processes shown in the flowchart, the image is segmented into regions by hue in the image. Figures 7 and 8 show the results of color segmentation. The image in Fig. 7 was segmented into three main regions and remaining regions, and the image in Fig. 8 was segmented into five main regions and remaining regions.

Confusion-line judgment block

This block is to judge whether the regions obtained through the color-segmentation block are located on the same confusion line. First, RGB data is converted into $L_pM_pS_p$ values for protanopes and $L_dM_dS_d$ values for deuteranopes after going through the CVD simulation process presented by Viénot et al.[6] Each R, G, B 3-D space[10] is divided into eight units, and eight each of R, G, and B are made for a total of 512 virtual boxes. Then, after going through the color-recognition simulation process presented by Viénot et al.,[6] the virtual boxes that belong to the same confusion line are mapped into the same group. Using this process, all of the boxes located in the same confusion line are grouped. These are then labeled P1, P2, P3, …, P52 for the same confusion lines to make a confusion-line map for protanopia. In the case of deuteranopia, D1 ∼ D41 groups are established. Table I shows a CVD confusion-line map. Table I includes some confusion lines, but Tables A.1 and A.2 including all confusion-line groups (i.e., the 52 confusion lines for protanopia and the 41 confusion lines for deuteranopia) are attached in the appendix at the end of the article.

Figure 9 shows some confusion lines of protanopia in the CIE XYZ space.[11] Figure 10 shows some confusion lines of protanopia and deuteranopia in the CIE 1931

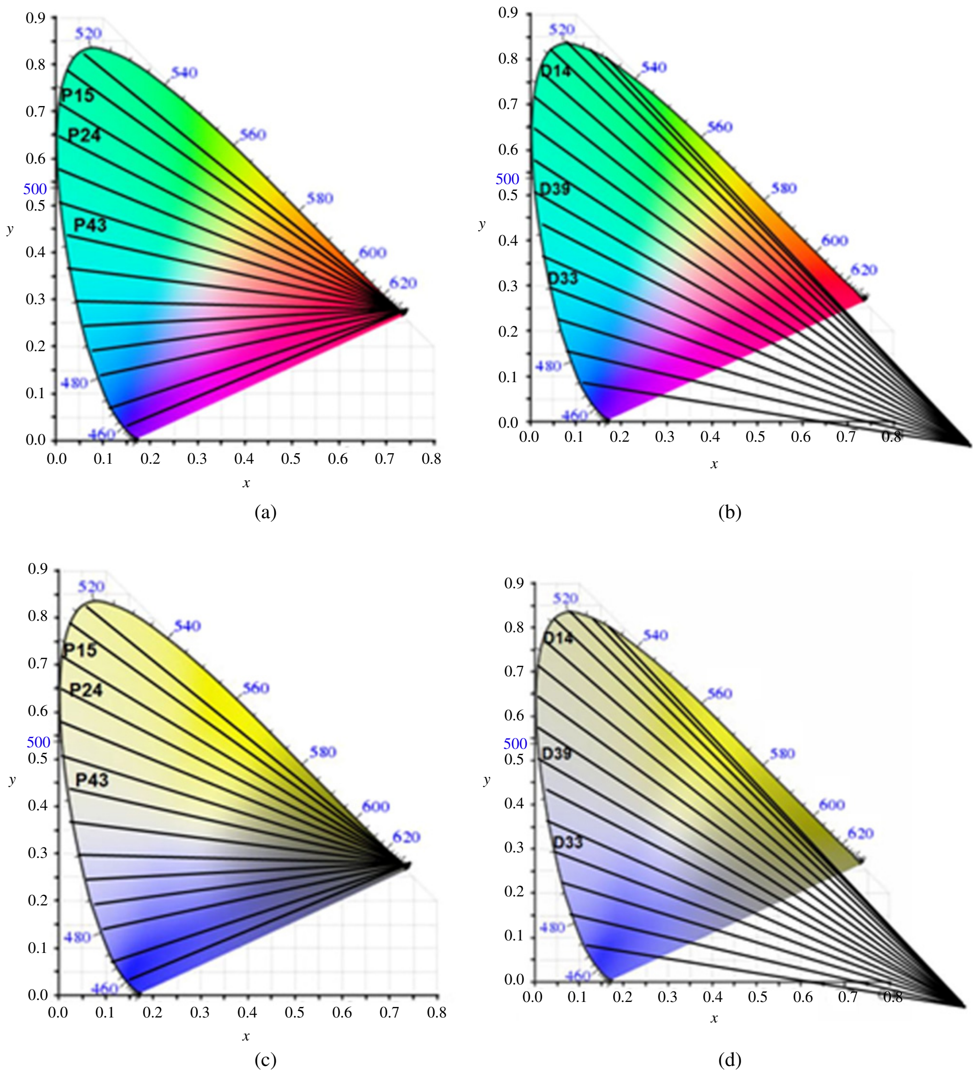

Figure 10. Confusion lines in the CIE 1931 chromaticity diagram. (a) Confusion lines of protanopia. (b) Confusion lines of deuteranopia. (c) Simulation image as perceived by a protanope. (d) Simulation image as perceived by a deuteranope.

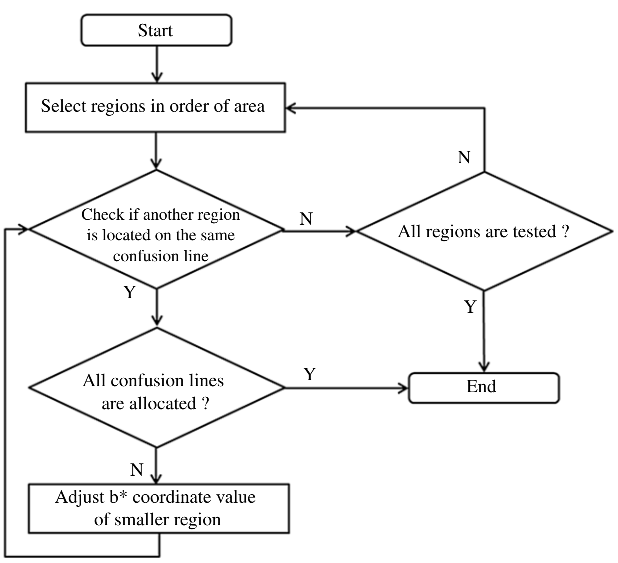

Figure 11. CIE Lab color-space color-adjustment flowchart.

chromaticity diagram.[12] Image 10(a) shows some confusion lines of protanopia, and (b) shows some confusion lines of deuteranopia in the CIE 1931 chromaticity diagram. Colors lying on the same confusion line are perceived by individuals with red–green CVD as having the same hue and colorfulness but are perceived as identical only at the right luminance ratio. Image (c) is the simulation image of (a) as perceived by a protanope. Image (d) is the simulation image of (b) as perceived by a deuteranope. For example, no hue values located on confusion line P15 can be distinguished by a protanope. In addition, no hue values located on confusion line D14 can be distinguished by a deuteranope.

CIE Lab color-space color-adjustment block

This block corrects colors in the segmented regions obtained from the color-segmentation block using the confusion-line map information obtained from the confusion-line judgment block for protanopia and deuteranopia. This block compares the hue information of all segmented regions

(a) Original image

(b) Simulation image as perceived by a protanope

(c) Simulation image as perceived by a deuteranope

(d) Recolored image for protanopia by proposed algorithm

(e) Simulation image of (d) as perceived by a protanope

(f) Recolored image for deuteranopia by proposed algorithm

(g) Simulation image of (f) as perceived by a deuteranope

Figure 12. Experimental results.

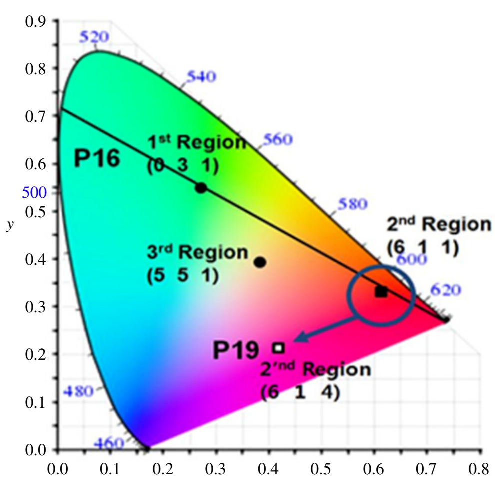

(a) CIE 1931 color-coordinate system

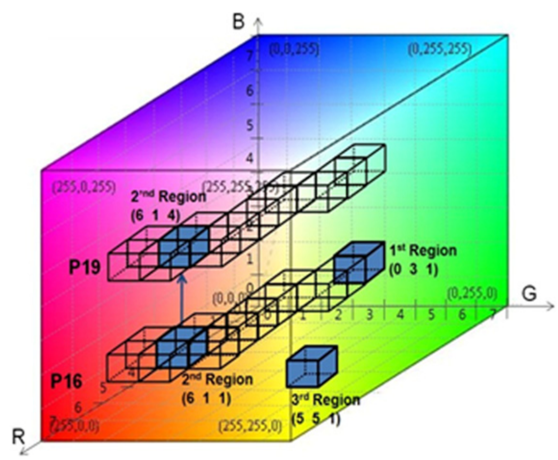

(b) RGB color space

Figure 13. Results of separation in confusion line in CIE 1931 color-coordinate system and RGB color space.

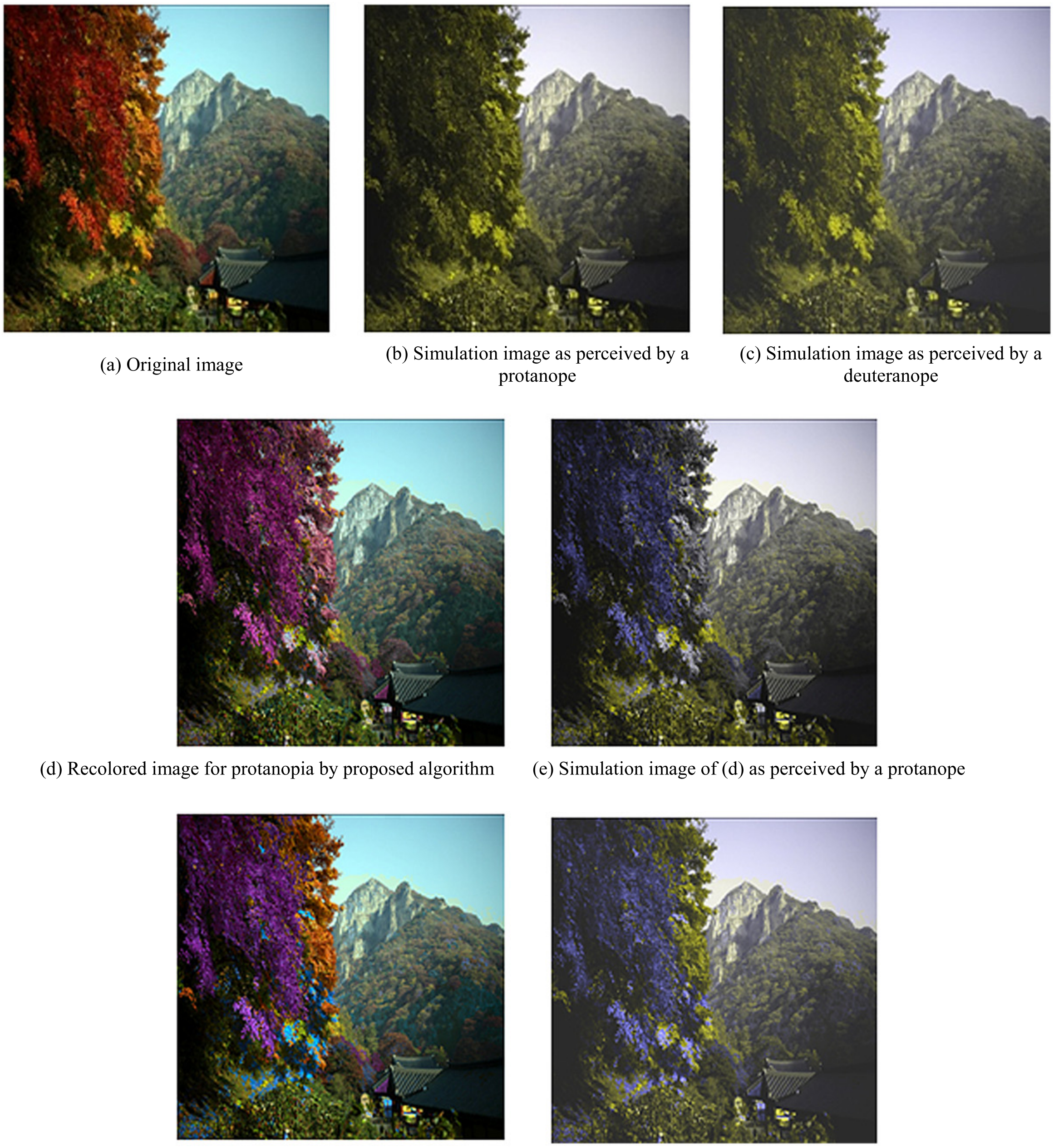

(a) Original image

(b) Simulation image as perceived by a protanope

(c) Simulation image as perceived by a deuteranope

(d) Recolored image for protanopia by proposed algorithm

(e) Simulation image of (d) as perceived by a protanope

(f) Recolored image for deuteranopia by proposed algorithm

(g) Simulation image of (f) as perceived by a deuteranope

Figure 14. Experimental results.

and converts the hue of any regions located on the same confusion line so that they go out of the confusion line until all the corrected hue values are located on a different confusion line or there is no remaining confusion line to go out. Figure 11 shows a flowchart of the CIE Lab color-space color-adjustment block. This block converts the RGB signals on the same confusion line handed over from the confusion-line judgment block into CIE L*a*b* signals. The a* coordinate of CIE L*a*b* corresponds approximately to the dimensions of redness–greenness. The b* coordinate corresponds approximately to the dimensions of yellowness–blueness. Therefore, the hue of any regions located on the same confusion line can leave the confusion line very easily by changing the b* coordinate value in CIE L*a*b*. As shown in Fig. 11, if the two regions are located on the same confusion line, the b* coordinate value of the smaller region is adjusted so that corrected color regions are kept to a minimum. This block adjusts the b* coordinate value of the selected region and converts the signals into RGB signals. After that, this block again judges whether the regions are on the same confusion line. If some regions are still on the same confusion line, this block applies the confusion-line

Table II. Results of confusion-line separation.

Image	Confusion-line mapping				
	Confusing hue regions (Region : hue)	Before separation	Simulation image as perceived by a protanope	After separation	Simulation image as perceived by a protanope
	R1 : 180 R2 : 50	P15 (1, 3, 0) P15 (6, 1, 0)		P15 (1, 3, 0) P20 (6, 1, 5)	
	R1 : 126 R2 : 44 R3 : 182 R4 : 220 R5 : 78	P24 (0, 4, 1) P24 (7, 2, 1) P12 (0, 1, 4) P21 (0, 3, 7) P32 (4, 4, 1)		P24 (0, 4, 1) P27 (7, 2, 4) P12 (0, 1, 4) P21 (0, 3, 7) P32 (4, 4, 1)	
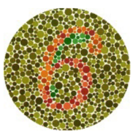	R1 : 124 R2 : 52	P23 (1, 4, 0) P23 (7, 2, 0)	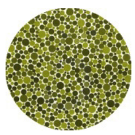	P23 (1, 4, 0) P29 (7, 2, 5)	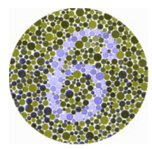
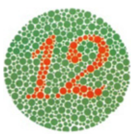	R1 : 112 R2 : 20	P15 (1, 3, 0) P15 (5, 2, 0)	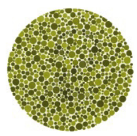	P15 (1, 3, 0) P19 (5, 2, 4)	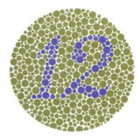
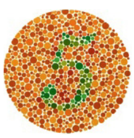	R1 : 50 R2 : 134	P34 (7, 4, 3) P34 (3, 5, 3)	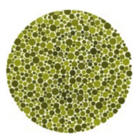	P34 (7, 4, 3) P36 (3, 5, 5)	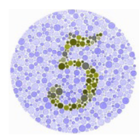
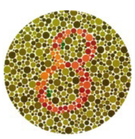	R1 : 135 R2 : 66	P43 (1, 6, 4) P43 (7, 5, 4)	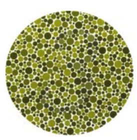	P43 (1, 6, 4) P45 (7, 5, 7)	
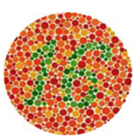	R1 : 46 R2 : 130	P23 (7, 3, 0) P23 (0, 4, 0)	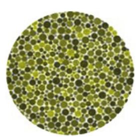	P23 (7, 3, 0) P27 (0, 4, 4)	
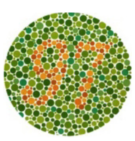	R1 : 132 R2 : 34	P42 (1, 6, 3) P42 (7, 5, 3)	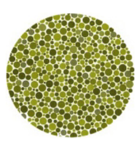	P42 (1, 6, 3) P45 (7, 5, 7)	

separation function again to repeat this process until all the regions are located on different confusion lines.

EXPERIMENTAL RESULTS

Figures 12 and 14 show the results of experiments conducted with general images. Fig. 12(a) is segmented into the three regions (b), (c), and (d) in Fig. 7. Fig. 7(b) shows the region of largest area and represents green-colored regions such as the green grass on the soccer field. This color region is mapped into the (0 3 1) virtual box and located on the P16 confusion line, as listed in Table A.1. Fig. 7(c) shows the second largest region and represents red-colored regions such as the t-shirts and socks of the soccer team members. This color region is mapped into the (6 1 1) virtual box and located on the same confusion line P16 in Table A.1. Fig. 7(d) shows the third region, which is mapped into the (5 5 1) virtual box. Figure 13(a) shows the positions of three color regions in the CIE 1931 color-coordinate system and shows that among these three regions, the first and second region

Table III. Results of confusion-line separation in CIE 1931.

Image	Results of confusion-line separation in CIE 1931	Image	Results of confusion-line separation in CIE 1931
	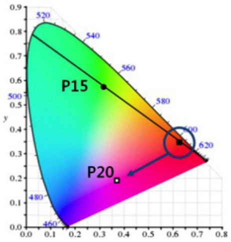		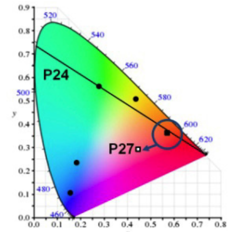
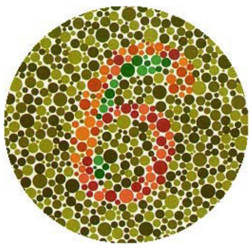	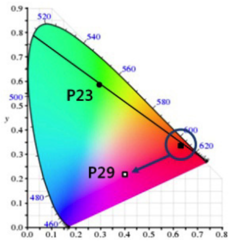	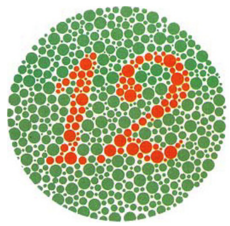	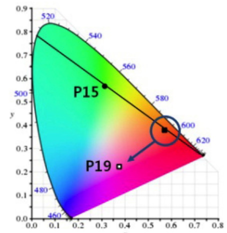
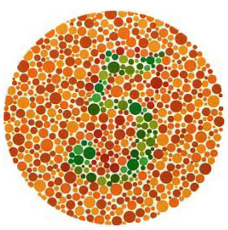	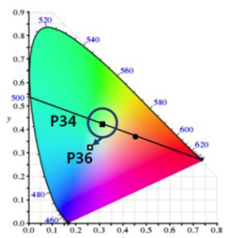	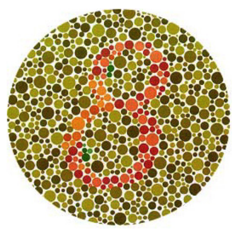	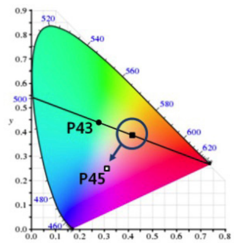
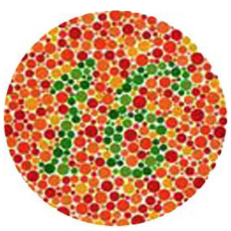	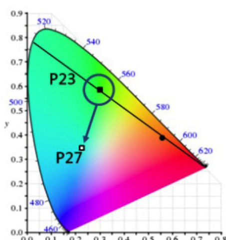	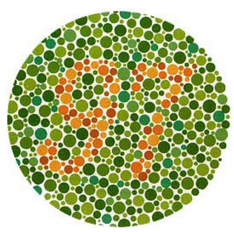	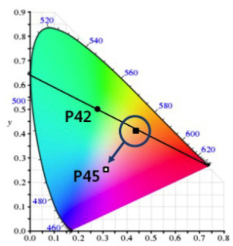

exist on the same confusion line (P16). Therefore, color adjustment for differentiating between the first and second regions is performed in the color-adjustment block. The results of the experiments revealed that all three regions were located on different confusion lines (P16, P19, and P40), and thus, optimum color-correction effects could be provided to people with CVDs. Fig. 13(b) shows the confusion lines and separation process representing the RGB color space. Fig. 12(e) and (g) and Fig. 14(e) and (g) show the simulation images as perceived by a protanope and a deuteranope after recoloring by the proposed algorithm. According to the results of the simulation, observers with CVDs would make fewer color-discrimination mistakes when viewing these images.

Table II shows the results of confusion-line separation using diverse images that have confusing color regions. After processing the proposed algorithm, all confusing regions are located on the different confusion lines.

Table III shows the results of separation in the CIE 1931 color-coordinate system. It offers a visual representation of the confusion-line separation results presented in Table II. The regions located in the same confusion line are separated into the different confusion lines.

Table IV. Test image set samples.

No	Original image	(a) Daltonization[2]	(b) Chen et al.[5]	(c) Proposed method
1				
2				
14				
23		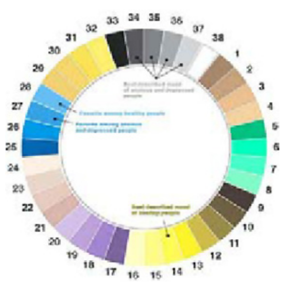	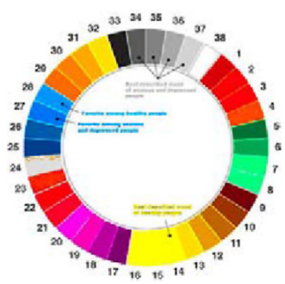	
33	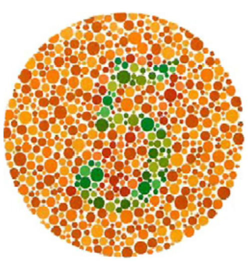	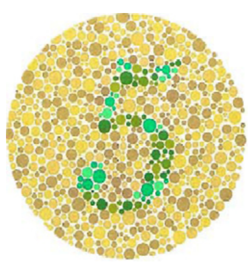	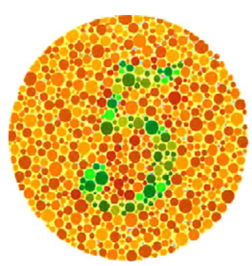	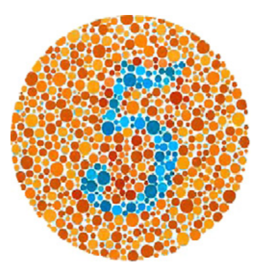

In the previous color-perception simulation for CVDs, experimental results were shown through the algorithm proposed by Viénot et al.[6] Finally, actual participants with CVDs were recruited to verify the performance of the proposed algorithm.

The performance of the proposed algorithm was compared with that of Daltonization,[2] the most widely known of the CVD color-correction algorithms, and that of Chen et al.'s[5] algorithm, which was recently proposed. In the experiment, 38 carefully selected images, such as Ishihara

Table V. Results of the choice through the 3-AFC method.

	(a) Daltonization[2]		(b) Chen et al.[5]		(c) Proposed method	
A	6/38	15.8%	14/38	36.8%	18/38	47.4%
B	4/38	10.5%	9/38	23.7%	25/38	65.8%
C	9/38	23.7%	9/38	23.7%	20/38	52.6%
D	5/38	13.2%	7/38	18.4%	26/38	68.4%
E	8/38	21.1%	10/38	26.3%	20/38	52.6%
F	9/38	23.7%	6/38	15.8%	23/38	60.5%
G	8/38	21.1%	9/38	23.7%	21/38	55.2%
H	6/38	15.8%	9/38	23.7%	23/38	60.5%
I	13/38	34.2%	2/38	5.3%	23/38	60.5%
J	12/38	31.6%	3/38	7.9%	23/38	60.5%
Average	8.0/38	21.1%	7.8/38	20.5%	22.2/38	58.4%

test images and other images frequently used in color-image processing, were recolored through the three algorithms. In addition, the resultant 38 image sets were provided after covering the names of the algorithms to conduct blind tests. Table IV shows the five sample image sets of the 38 test image sets used in the test.

The test was conducted using the 3-AFC (3-alternative forced-choice) method.[13] The 10 participants with CVDs (diagnosed with protanomaly in a yearly medical examination) were 11th-grade male high school students (age 17). They were asked to unconditionally select the image with the largest color-separating effect from three given images. Table V presents the results of the 38 test sets conducted using the 3-AFC method. The names of the individuals with CVDs were not disclosed and were referred to as A to J. The results of the test showed that the results of the algorithm proposed in this article were the best. Furthermore, the other algorithms were shown to modify the overall color of test images. However, the proposed algorithm preserved most of the colored region and merely modified the color region confused by individuals with CVDs.

This table shows that 58.4% (on average) of the 10 individuals with CVDs preferred the proposed algorithm. Figure 15 shows the results of the test organized in a chart.

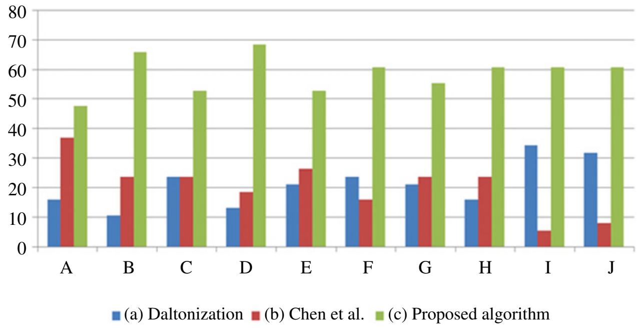

Figure 15. Results of the choice through the 3-AFC method.

CONCLUSIONS

In this study, we proposed a confusion-line separation algorithm using color-region segmentation for red–green CVDs. Most previous color-conversion methods changed entire images globally into RGB or CIELAB color spaces or adjusted signals from LMSs to perform color correction. In such cases, conventional algorithms modified the overall color of image regions.

To relieve these disadvantages, a more detailed and optimal correction method is proposed in this article. Input images were segmented into regions by hue, and the existence of confusions among the segmented regions was checked. If any regions were located on the same confusion line, color adjustment was performed to ensure all the segmented regions were located on different confusion lines. The confusion-line map for judging whether regions were on the same confusion line was made more accessible by making virtual boxes in a 3-D RGB space. A total of 512 virtual boxes were made in an RGB space. After going through the color-recognition simulation process presented by Viénot et al.[6] the virtual boxes that belonged to the same confusion line were mapped into the same group. In total, 52 confusion-line groups for protanopia and 41 confusion-line groups for deuteranopia were made in predetermined table form. These tables were used to locate color-confusion regions in an image and to verify that all regions were located on different confusion lines.

In order to verify the performance of the proposed algorithm, a clinical test of two existing color-correction algorithms and the proposed algorithm was conducted with participants with CVDs using the 3-AFC method. The results revealed that the performance of the proposed algorithm was identified to be the best. Furthermore, the proposed algorithm was shown to preserve the color of most regions. Therefore, after the color correction, most color regions remained unchanged, and the color difference between the original image and the color-corrected image of the proposed algorithm was kept to a minimum. The color-corrected images generated by the proposed algorithm could be seen by trichromats and anomalous trichromats simultaneously with less inconvenience.

ACKNOWLEDGMENTS

This work was supported by a National Research Foundation of Korea Grant funded by the Korean Government (No. 2012-007498) and by IDEC Platform Center (IPC). And this work was also supported by the ETRI R&D Program of KCC (Korea Communications Commission), Korea [11921-03001, “Development of Beyond Smart TV Technology”].

Appendix

See Tables A.1 and A.2.

Table A.1. Confusion-line map for protanopia.

Type of confusion line	Representative box position (R G B)	Box positions in same confusion line (R G B)							
P1	000	000	100	200					
P2	001	001	101	201					
P3	002	002	102	202					
P4	003	003	103	203					
P5	004	004	104	204					
P6	005	005	006	105	106	205	206		
P7	007	007	107	207					
P8	110	010	020	110	120	210	300	310	400
		410	500						
P9	111	011	021	111	121	211	301	311	401
		411	501						
P10	112	012	022	112	122	212	302	312	402
		412	502						
P11	113	013	023	113	123	213	303	313	403
		413	503						
P12	114	014	024	114	124	214	304	314	404
		414	504						
P13	115	015	016	025	026	115	116	125	126
		215	216	305	315	405	415	505	
P14	117	017	027	117	127	217	306	307	316
		317	406	407	416	417	506	507	
P15	220	030	130	220	230	320	420	510	520
		600	610	620	700	710			
P16	221	031	131	221	231	321	421	511	521
		601	611	621	701	711			
P17	222	032	132	222	232	322	422	512	522
		602	612	622	702	712			
P18	223	033	133	223	233	323	423	513	523
		603	613	623	703	713			
P19	224	034	134	224	234	324	424	514	524
		604	614	624	704	714			
P20	225	035	036	135	136	225	226	235	236
		325	326	425	515	525	605	615	625
		705	715						
P21	227	037	137	227	237	327	426	427	516
		517	526	527	606	616	626	627	706
		716							
P22	607	607	617	707	717				
P23	330	040	140	240	330	340	430	530	630
		720	730						
P24	331	041	141	241	331	341	431	531	631
		721	731						

(*continued on next page*)

Table A.1. (*continued*)

Type of confusion line	Representative box position (R G B)	Box positions in same confusion line (R G B)							
P25	3 3 2	0 4 2	1 4 2	2 4 2	3 3 2	3 4 2	4 3 2	5 3 2	6 3 2
		7 2 2	7 3 2						
P26	3 3 3	0 4 3	1 4 3	2 4 3	3 3 3	3 4 3	4 3 3	5 3 3	6 3 3
		7 2 3	7 3 3						
P27	3 3 4	0 4 4	1 4 4	2 4 4	3 3 4	3 4 4	4 3 4	5 3 4	6 3 4
		7 2 4	7 3 4						
P28	3 3 5	0 4 5	0 4 6	1 4 5	1 4 6	2 4 5	2 4 6	3 3 5	3 3 6
		3 4 5	3 4 6	4 3 5	5 3 5	6 3 5	7 2 5	7 3 5	
P29	3 3 7	0 4 7	1 4 7	2 4 7	3 3 7	3 4 7	4 3 6	4 3 7	5 3 6
		5 3 7	6 3 6	6 3 7	7 2 6	7 3 6			
P30	7 2 7	7 2 7	7 3 7						
P31	4 4 0	0 5 0	1 5 0	2 5 0	3 5 0	4 4 0	4 5 0	5 4 0	6 4 0
		7 4 0							
P32	4 4 1	0 5 1	1 5 1	2 5 1	3 5 1	4 4 1	4 5 1	5 4 1	6 4 1
		7 4 1							
P33	4 4 2	0 5 2	1 5 2	2 5 2	3 5 2	4 4 2	4 5 2	5 4 2	6 4 2
		7 4 2							
P34	4 4 3	0 5 3	1 5 3	2 5 3	3 5 3	4 4 3	4 5 3	5 4 3	6 4 3
		7 4 3							
P35	4 4 4	0 5 4	0 5 5	1 5 4	1 5 5	2 5 4	2 5 5	3 5 4	4 4 4
		4 5 4	5 4 4	6 4 4	7 4 4				
P36	4 4 5	0 5 6	1 5 6	2 5 6	3 5 5	3 5 6	4 4 5	4 4 6	4 5 5
		4 5 6	5 4 5	6 4 5	7 4 5				
P37	4 4 7	0 5 7	1 5 7	2 5 7	3 5 7	4 4 7	4 5 7	5 4 6	5 4 7
		6 4 6	6 4 7	7 4 6					
P38	7 4 7	7 4 7							
P39	5 5 0	0 6 0	1 6 0	2 6 0	3 6 0	4 6 0	5 5 0	5 6 0	6 5 0
		6 6 0	7 5 0						
P40	5 5 1	0 6 1	1 6 1	2 6 1	3 6 1	4 6 1	5 5 1	5 6 1	6 5 1
		6 6 1	7 5 1						
P41	5 5 2	0 6 2	1 6 2	2 6 2	3 6 2	4 6 2	5 5 2	5 6 2	6 5 2
		6 6 2	7 5 2						
P42	5 5 3	0 6 3	1 6 3	2 6 3	3 6 3	4 6 3	5 5 3	5 6 3	6 5 3
		6 6 3	7 5 3						
P43	5 5 4	0 6 4	0 6 5	1 6 4	1 6 5	2 6 4	2 6 5	3 6 4	3 6 5
		4 6 4	4 6 5	5 5 4	5 6 4	6 5 4	6 6 4	7 5 4	
P44	5 5 5	0 6 6	1 6 6	2 6 6	3 6 6	4 6 6	5 5 5	5 5 6	5 6 5
		5 6 6	6 5 5	6 6 5	6 6 6	7 5 5			
P45	5 5 7	0 6 7	1 6 7	2 6 7	3 6 7	4 6 7	5 5 7	5 6 7	6 5 6
		6 5 7	6 6 7	7 5 6	7 5 7				

(*continued on next page*)

Table A.1. (*continued*)

Type of confusion line	Representative box position (R G B)	Box positions in same confusion line (R G B)							
P46	670	070	170	270	370	470	570	670	760
		770							
P47	671	071	171	271	371	471	571	671	761
		771							
P48	672	072	172	272	372	472	572	672	762
		772							
P49	673	073	074	173	174	273	274	373	374
		473	573	673	763	773			
P50	674	075	175	275	375	474	475	574	575
		674	764	774					
P51	675	076	176	276	376	476	576	675	676
		765	775	776					
P52	777	077	177	277	377	477	577	678	766
		767	777						

Table A.2. Confusion-line map for deuteranopia.

Type of confusion line	Representative box position (R G B)	Box positions in same confusion line (R G B)							
D1	111	000	001	010	011	100	101	110	111
		200	201	210	211				
D2	112	002	012	102	112	202	212		
D3	113	003	013	103	113	203	213		
D4	114	004	014	104	114	204	214		
D5	115	005	006	015	016	105	106	115	116
		205	206	215	216				
D6	117	007	017	107	117	207	217		
D7	221	020	021	030	031	120	121	130	131
		220	221	230	231	300	301	310	311
		320	321	400	401	410	411	420	421
D8	222	022	032	122	132	222	232	302	312
		322	402	412	422				
D9	223	023	033	123	133	223	233	303	313
		323	403	413	423				
D10	224	024	034	124	134	224	234	304	314
		324	404	414	424				
D11	225	025	026	035	125	126	135	225	226
		235	236	305	306	315	316	325	326
		405	406	415	416	425	426		
D12	227	027	036	037	127	136	137	227	237
		307	317	327	407	417	427		
D13	600	600	610						

(*continued on next page*)

Table A.2. (*continued*)

Type of confusion line	Representative box position (R G B)	Box positions in same confusion line (R G B)							
D14	3 3 1	0 4 0	0 4 1	1 4 0	1 4 1	2 4 0	2 4 1	3 3 0	3 3 1
		3 4 0	3 4 1	4 3 0	4 3 1	5 0 0	5 0 1	5 1 0	5 1 1
		5 2 0	5 2 1	5 3 0	5 3 1	6 0 1	6 1 1	6 2 0	6 2 1
D15	3 3 2	0 4 2	1 4 2	2 4 2	3 3 2	3 4 2	4 3 2	5 0 2	5 1 2
		5 2 2	5 3 2	6 0 2	6 1 2	6 2 2			
D16	3 3 3	0 4 3	1 4 3	2 4 3	3 3 3	3 4 3	4 3 3	5 0 3	5 1 3
		5 2 3	5 3 3	6 0 3	6 1 3	6 2 3			
D17	3 3 4	0 4 4	1 4 4	2 4 4	3 3 4	3 4 4	4 3 4	5 0 4	5 0 5
		5 1 4	5 1 5	5 2 4	5 2 5	5 3 4	6 0 4	6 0 5	6 1 4
		6 1 5	6 2 4	6 2 5					
D18	3 3 5	0 4 5	1 4 5	2 4 5	3 3 5	3 3 6	3 4 5	4 3 5	4 3 6
		5 0 6	5 1 6	5 2 6	5 3 5	5 3 6	6 0 6	6 1 6	6 2 6
D19	3 3 7	0 4 6	0 4 7	1 4 6	1 4 7	2 4 6	2 4 7	3 3 7	3 4 6
		3 4 7	4 3 7	5 0 7	5 1 7	5 2 7	5 3 7	6 0 7	6 1 7
		6 2 7							
D20	7 0 0	7 0 0	7 1 0	7 2 0	7 3 0				
D21	4 4 1	0 5 0	0 5 1	1 5 0	1 5 1	2 5 0	2 5 1	3 5 0	3 5 1
		4 4 0	4 4 1	4 5 0	4 5 1	5 4 0	5 4 1	6 3 0	6 3 1
		6 4 0	6 4 1	7 0 1	7 1 1	7 2 1	7 3 1		
D22	4 4 2	0 5 2	1 5 2	2 5 2	3 5 2	4 4 2	4 5 2	5 4 2	6 3 2
		6 4 2	7 0 2	7 1 2	7 2 2	7 3 2			
D23	4 4 3	0 5 3	1 5 3	2 5 3	3 5 3	4 4 3	4 5 3	5 4 3	6 3 3
		6 4 3	7 0 3	7 0 4	7 1 3	7 1 4	7 2 3	7 2 4	7 3 3
		7 3 4							
D24	4 4 4	0 5 4	1 5 4	2 5 4	3 5 4	4 4 4	4 5 4	5 4 4	6 3 4
		6 3 5	6 4 4	6 4 5	7 0 5	7 1 5	7 2 5	7 3 5	
D25	4 4 5	0 5 5	1 5 5	2 5 5	3 5 5	4 4 5	4 4 6	4 5 5	5 4 5
		5 4 6	6 3 6	6 4 6	7 0 6	7 1 6	7 2 6	7 3 6	
D26	4 4 7	0 5 6	0 5 7	1 5 6	1 5 7	2 5 6	2 5 7	3 5 6	3 5 7
		4 4 7	4 5 6	4 5 7	5 4 7	6 3 7	6 4 7	7 0 7	7 1 7
		7 2 7	7 3 7						
D27	7 4 0	7 4 0							
D28	5 5 1	0 6 0	0 6 1	0 7 0	0 7 1	1 6 0	1 6 1	1 7 0	1 7 1
		2 6 0	2 6 1	3 6 0	3 6 1	4 6 0	4 6 1	5 5 0	5 5 1
		5 6 0	5 6 1	6 5 0	6 5 1	6 6 0	6 6 1	7 4 1	7 5 0
D29	5 5 2	0 6 2	0 7 2	1 6 2	1 7 2	2 6 2	3 6 2	4 6 2	5 5 2
		5 6 2	6 5 2	6 6 2	7 4 2	7 5 2			
D30	5 5 3	0 6 3	0 7 3	1 6 3	1 7 3	2 6 3	3 6 3	4 6 3	5 5 3
		5 6 3	6 5 3	6 6 3	7 4 3	7 5 3			
D31	5 5 4	0 6 4	0 7 4	1 6 4	1 7 4	2 6 4	3 6 4	4 6 4	5 5 4
		5 6 4	6 5 4	6 6 4	7 4 4	7 4 5	7 5 4	7 5 5	

(*continued on next page*)

Table A.2. (*continued*)

Type of confusion line	Representative box position (R G B)	Box positions in same confusion line (R G B)							
D32	5 5 5	0 6 5	0 7 5	1 6 5	1 7 5	2 6 5	3 6 5	4 6 5	5 5 5
		5 6 5	6 5 5	6 5 6	6 6 5	6 6 6	7 4 6	7 5 6	
D33	5 5 7	0 6 6	0 7 6	1 6 6	1 7 6	2 6 6	2 6 7	3 6 6	3 6 7
		4 6 6	4 6 7	5 5 7	5 6 6	5 6 7	6 5 7	6 6 7	7 4 7
		7 5 7							
D34	1 7 7	0 6 7	0 7 7	1 6 7	1 7 7				
D35	7 7 1	2 7 0	2 7 1	3 7 0	3 7 1	4 7 0	4 7 1	5 7 0	5 7 1
		6 7 0	6 7 1	7 6 0	7 6 1	7 7 0	7 7 1		
D36	7 7 2	2 7 2	3 7 2	4 7 2	5 7 2	6 7 2	7 6 2	7 7 2	
D37	7 7 3	2 7 3	3 7 3	4 7 3	5 7 3	6 7 3	7 6 3	7 7 3	
D38	7 7 4	2 7 4	3 7 4	4 7 4	5 7 4	6 7 4	7 6 4	7 7 4	
D39	7 7 5	2 7 5	3 7 5	4 7 5	5 7 5	6 7 5	7 6 5	7 6 6	7 7 5
		7 7 6							
D40	7 7 7	2 7 6	3 7 6	4 7 6	5 7 6	5 7 7	6 7 6	6 7 7	7 6 7
		7 7 7							
D41	4 7 7	2 7 7	3 7 7	4 7 7					

REFERENCES

[1] M. P. Simunovic, "Color vision deficiency," Eye **24**, 747–755 (2010).
[2] C. Anagnostopoulos, G. T. Ouras, I. Anagnostopoulos, and C. Kalloniatis, "Intelligent modification for the Daltonization process of digitized paintings," *ICVS* (2007).
[3] J. B. Huang, Y. C. Tseng, S. I. Wu, and S. J. Wang, "Information preserving color transformation for protanopia and deuteranopia," IEEE Signal Process. Lett. **14**, 711–714 (2007).
[4] B. Liu, M. Wang, L. Yang, X. Wu, and X. Hua, "Efficient image and video re-coloring for colorblindness," *ICME*, 906–909 (2009).
[5] Y. Chen and T. Liao, "Hardware digital color enhancement for color vision deficiencies," ETRI J. **33**, (2011).
[6] F. Viénot, H. Brettel, and J. Mollon, "Digital video colourmaps for checking the legibility of displays by dichromats," Color Res. Appl. **24**, 243–252 (1999).
[7] P. Green and L. MacDonald, *Colour Engineering Achieving Device Independent Colour* (John Wiley & Sons, Chichester, UK, 2002).
[8] C. Poynton, *Digital Video and HDTV Algorithms and Interfaces* (Elsevier Science, San Francisco, 2003).
[9] C. I. R. Adams and L. Bischof, "Seeded region growing," IEEE Trans. Pattern Anal. Mach. Intell. **16**, 641–647 (1994).
[10] D. Han, "Real-time color gamut mapping method for digital TV display quality enhancement," IEEE Trans. Consum. Electron. **50**, 691–699 (2004).
[11] G. W. Meyer and D. P. Greenberg, "Color-defective vision and computer graphics displays," IEEE Comput. Graph. Appl. **8**, 28–40 (1988).
[12] CIE, "Uniform color spaces — Color difference equations psychometric color terms," Commission Internationale de L'Eclairage **15**, (1978).
[13] D. Roberson and J. Davidoff, "The categorical perception of colors and facial expressions: The effect of verbal interference," Mem. Cognition **28**, 977–986 (2000).